Open Journal of Geology, 2012, 2, 229-240
http://dx.doi.org/10.4236/ojg.2012.24023 Published Online October 2012 (http://www.SciRP.org/journal/ojg)

U-Pb Zircon Age, Geochemical and Sr-Nd Isotopic Constraints on the Age and Origin of the Granodiorites in Guilong, Southeastern Yunnan Province, Southern China

Shen Liu[1], Ruizhong Hu[1], Caixia Feng[1], Shan Gao[2], Guangying Feng[1], Youqiang Qi[1], Tao Wang[3], Ian M. Coulson[4], Yuhong Yang[1], Chaogui Yang[1]
[1]State Key Laboratory of Ore Deposit Geochemistry, Institute of Geochemistry, Chinese Academy of Sciences, Guiyang, China
[2]State Key Laboratory of Geological Processes and Mineral Resources, China University of Geosciences, Wuhan, China
[3]Chengdu University of Technology, Chengdu, China
[4]Solid Earth Studies Laboratory, Department of Geology, University of Regina, Regina, Canada
Email: liushen@vip.gyig.ac.cn

Received July 9, 2012; revised August 6, 2012; accepted September 7, 2012

ABSTRACT

Post-collision felsic rocks in Southeastern Yunnan province contain granodiorites. U-Pb zircon ages, geochemical data and Sr-Nd isotopic data for these rocks are reported in the present paper. Laser ablation inductively coupled plasma mass spectrometry U-Pb zircon analyses yielded consistent age 252.5 ± 1.0 Ma for one sample of the felsic rocks. The granodiorites were characterized by variational and high $(^{87}Sr/^{86}Sr)_i$, ranging from 0.7223 to 0.7236 and very low $\varepsilon_{Nd}(t)$ values from –29.1 to –30.4. In addition, these rocks are characterized by slight Eu negative anomalies, Nb, Ta, Ti and Sr negative anomalies on primitive mantle normalization spider. Geochemical and isotopic characteristics suggest that these rocks were derived from an enriched crust source. The granodiorites resulted from the fractionation of potassium feldspar, plagioclase and ilmenite or rutile. However, the granodiorites were unaffected by visible crustal contamination during ascent. As a result, the granodiorites may have been formed due to partial melting of crust-derived sedimentary rocks beneath southeastern Yunnan province, southern China.

Keywords: Granodiorites; Age; Origin; Southeastern Yunnan Province; Southern China

1. Introduction

Felsic rocks (e.g., granite, granodiorite, etc.) are widely distributed in Honghe polymetallic deposits (super-large Sn, Cu, Pb, Zn, Sb, Ag, Mo, Au and Bi deposits) [1-6] and Bainiuchang super-large Ag-Pb-Zn polymetallic deposits [7-14]. These rocks, especially granite and granodiorite, can be used to study the mineralization and metallogenesis of polymetallic deposits in southeastern Yunnan province, Southern China.

Although a number of studies about deposits have been carried out, recent analytical techniques and systematic geochemical studies (e.g., ages, geochemical data and isotopic data) on granites and granodiorites are limited. Therefore, we provide systematic geochemical data and **LA-ICP-MS** zircon U-Pb and Sr-Nd data for the granodiorites to constrain age, source, fractionation and genetic model of the studied felsic rocks.

2. Geological Setting and Petrography

Many types of Mesozoic-Cenozoic granites and acidic porphyries are present in southeastern Yunnan province. Each felsic rock may provide important insights into the tectonothermal evolution of the Mesozoic-Cenozoic lithosphere of Yunnan province and the possible linkage(s) between Yunnan and other places (*i.e.*, terrene, craton, etc.). Limited precise ages for the felsic rocks in Yunnan province have been published in recent papers.

The study area is located within Guilong area, Luchun County, Yunnan province, southeastern China (**Figure 1**). Granodiorites in Guilong are emplaced into Trias sedimentary rocks (**T_3g**) (e.g., sandstone and shale) and granite without precise age. Some orthoclase and mafic dykes (x, lamprophyres) are present in the southern margin of the granodiorites. The granodiorites are commonly ~0.9 km wide and ~1.7 km long. They are exposed for ca. 1.6 km^2. The ages of these rocks remain unknown. **Figure 2** shows the representative photomicrographs of the granodiorites from Guilong. All granodiorites are porphyry with typical porphyritic texture and massive structure (**Figure 2**). The granodiorites mainly contain 40% to 45% plagioclase, 16% to 18% potash feldspar (K-feld-

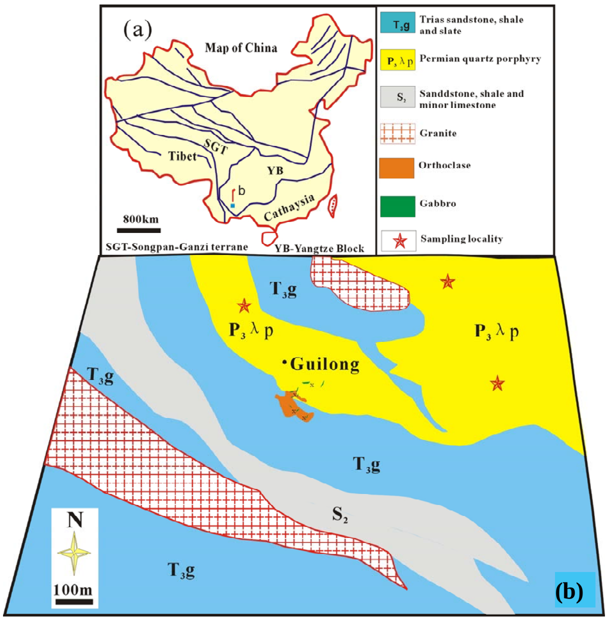

Figure 1. **(a) Simplified tectonic map of the study area, Yunnan Province, China; (b) Map of China and distributions of the fault.**

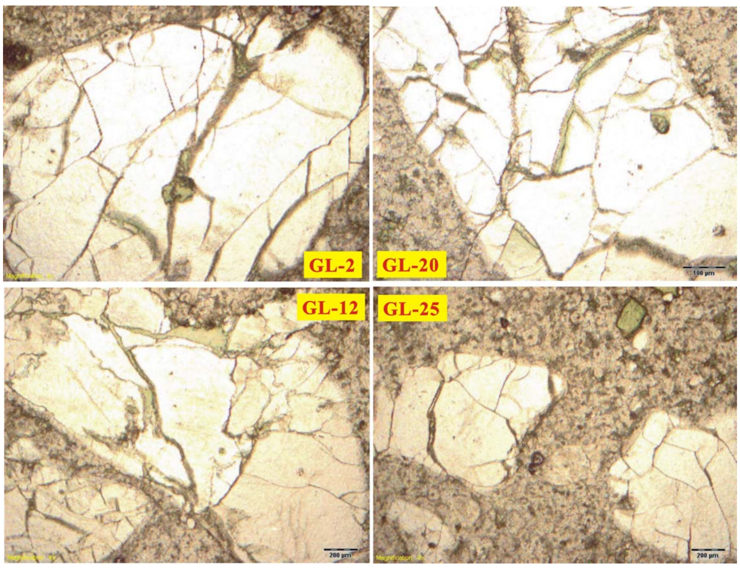

Figure 2. Repressive photos of granodiorites in Guilong, Southeastern Yunnan Province.

spar), 20% to 25% quartz, 5.0% to 8.0% biotite, 2.0% to 5.0% hornblende and minor (<2.0%) accessory minerals, such as apatite, titanite, zircon, magnetite, allanite, etc.

3. Analytical Procedures

3.1. U-Pb Dating by LA-ICP-MS Method

Zircon was separated from one sample (**GL01**) using conventional heavy liquid and magnetic techniques at the Langfang Regional Geological Survey, Hebei Province, China. Zircon separates were examined under transmitted and reflected light and by cathodoluminescence petrography at the State Key Laboratory of Continental Dynamics, Northwest University, China, to observe their external and internal structures.

Laser-ablation techniques were employed for zircon age determinations (**Table 1**; **Figure 3**) using an Agilent 7500a ICP-MS instrument equipped with a 193 nm excimer laser at the State Key Laboratory of Geological Processes and Mineral Resources, China University of Geoscience, Wuhan, China. Zircon #91500 was used as standard and NIST 610 was used to optimize the results. A spot diameter of 24 μm was used. Prior to LA-ICP-MS

Table 1. LA-ICPMS U-Pb isotopic data for zircons in the felsic rocks in Guilong, Yunnan Province, China.

GL01					Isotopic	ratios					Age(Ma)					
Spot	Th(ppm)	U(ppm)	Pb(ppm)	Th/U	$^{207}Pb/^{206}Pb$	1d	$^{207}Pb/^{235}U$	1d	$^{206}Pb/^{238}U$	1d	$^{207}Pb/^{206}Pb$	1d	$^{207}Pb/^{235}U$	1d	$^{206}Pb/^{238}U$	1d
1.1	53.3	390	17.2	0.14	0.0492	0.0014	0.2707	0.0078	0.0399	0.0003	167	60	243	6	252	2
2.1	77.5	295	13.5	0.26	0.0488	0.0017	0.2675	0.0092	0.0399	0.0003	200	81	241	7	252	2
3.1	132	460	21.5	0.29	0.0530	0.0021	0.2932	0.0116	0.0401	0.0003	328	91	261	9	253	2
4.1	72.0	305	13.9	0.24	0.0528	0.0019	0.2904	0.0109	0.0400	0.0004	320	114	259	9	253	3
5.1	63.1	302	13.7	0.21	0.0496	0.0015	0.2722	0.0082	0.0399	0.0004	176	75	244	7	252	2
6.1	132	454	21.1	0.29	0.0503	0.0014	0.2767	0.0076	0.0399	0.0003	209	95	248	6	252	2
7.1	111	363	17.1	0.31	0.0499	0.0015	0.2750	0.0082	0.0400	0.0003	191	70	247	7	253	2
8.1	55.2	249	11.4	0.22	0.0530	0.0019	0.2924	0.0106	0.0399	0.0004	332	77	260	8	252	2
9.1	115	405	18.8	0.28	0.0527	0.0019	0.2894	0.0097	0.0400	0.0004	317	80	258	8	253	2
10.1	67.0	317	14.5	0.21	0.0507	0.0015	0.2793	0.0080	0.0400	0.0003	233	67	250	6	253	2
11.1	168	355	17.3	0.47	0.0513	0.0033	0.2801	0.0174	0.0398	0.0007	254	148	251	14	252	4
12.1	106	367	17.2	0.29	0.0485	0.0017	0.2660	0.0088	0.0399	0.0003	124	84	239	7	252	2
13.1	137	353	119	0.39	0.1597	0.0026	5.4561	0.0880	0.2466	0.0015	2454	28	1894	14	**1421**	8
14.1	210	349	18.0	0.60	0.0498	0.0022	0.2750	0.0123	0.0400	0.0004	183	104	247	10	253	2
15.1	109	308	14.9	0.35	0.0499	0.0018	0.2750	0.0097	0.0399	0.0003	187	116	247	8	252	2
16.1	78.0	323	15.1	0.24	0.0511	0.0019	0.2814	0.0104	0.0399	0.0003	256	82	252	8	252	2
17.1	93.7	351	16.6	0.27	0.0506	0.0015	0.2792	0.0083	0.0399	0.0003	233	73	250	7	252	2
18.1	129	486	22.9	0.27	0.0536	0.0014	0.2963	0.0076	0.0400	0.0003	354	59	263	6	253	2
19.1	150	372	66.2	0.40	0.0712	0.0013	1.4415	0.0283	0.1463	0.0014	965	44	906	12	**880**	8
20.1	89.3	422	19.4	0.21	0.0505	0.0019	0.2808	0.0105	0.0400	0.0003	220	85	251	8	253	2

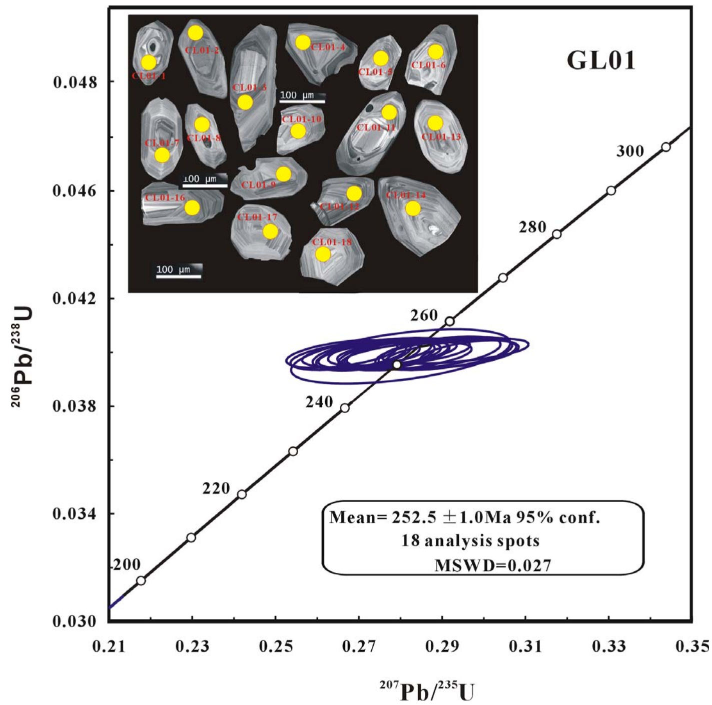

Figure 3. Selected zircon CL images and the LA-ICP-MS zircon U-Pb concordia diagram for the granodiorite (GL01) in Guilong, Southeastern Yunnan Province.

zircon U-Pb dating, the surfaces of the grain mounts were washed in dilute HNO_3 and pure alcohol to remove any potential lead contamination. The analytical methodology has been described in detail by Yuan *et al*. (2004) [15]. Correction for common Pb was performed following Andersen (2002) [16]. Data were processed using the GLITTER and ISOPLOT programs [17] (**Table 1**; **Figure 3**). Errors for individual analyses by LA-ICP-MS were quoted at the 95% (1σ) confidence level.

3.2. Major Elemental, Trace Elemental and Isotopic Analyses

Twenty-seven samples were collected to carry out major and trace element determinations and Sr-Nd isotopic analyses. Whole-rock samples were trimmed to remove altered surfaces, cleaned with deionized water and then crushed and powdered using an agate mill.

Major elements were analyzed using PANalytical Axios-advance (Axios PW4400) X-Ray Fluorescence spectrometer (**XRF**) at the State Key Laboratory of Ore Deposit Geochemistry, Institute of Geochemistry, Chinese Academy of Sciences. Fused glass disks were used. Based on the Chinese National standards GSR-1 and GSR-3 (**Table 2**), analytical precision was better than 5%. Loss on Ignition (**LOI**) was obtained using 1 g of powder heated to 1100˚C for 1 h.

Trace elements were analyzed by plasma optical emission MS ICP-MS at the National Research Center of Geoanalysis, Chinese Academy of Geosciences following the procedures described by Qi *et al*. (2000) [18]. The discrepancy among triplicates was less than 5% for all elements. Analysis results of the international standards OU-6 and GBPG-1 were consistent with the recommended values (**Table 3**).

For the analyses of Rb-Sr and Sm-Nd isotopes, sample powders were spiked with mixed isotope tracers, dissolved in Teflon capsules with HF + HNO_3 acids and separated by conventional cation-exchange techniques. Isotopic measurements were performed using a Finnigan Triton Ti thermal ionization mass spectrometer at the State Key Laboratory of Geological Processes and Mineral Resources, China University of Geosciences, Wuhan, China. Procedural blanks were <200 pg for Sm and Nd and <500 pg for Rb and Sr. Mass fractionation corrections for Sr and Nd isotopic ratios were based on $^{86}Sr/^{88}Sr = 0.1194$ and $^{146}Nd/^{144}Nd = 0.7219$, respectively. Analyses of standards yielded the following results: NBS987 gave $^{87}Sr/^{86}Sr = 0.710246 \pm 16$ (2σ) and La Jolla gave $^{143}Nd/^{144}Nd = 0.511863 \pm 8$ (2σ). The analyticcal results for Sr-Nd isotopes are presented in **Table 4**.

4. Results

4.1. Zircon U-Pb Age

Euhedral zircon grains in samples **GL01** are clean and prismatic, with magmatic oscillatory zoning. A total of 18 grains have a weighted mean $^{206}Pb/^{238}U$ age of 252.5 ± 1.0 Ma (1σ) (95% confidence interval) for **GL01** (**Ta-**

ble 1; **Figure 3**). These determinations are the best estimates of the crystallization ages of the granodiorites. Some inherited zircons (**1421 and 880 Ma**; **Table 1**) are present in the rock.

4.2. Major and Trace Elements

Geochemical data on the granodiorites in the study area are listed in **Tables 2** and **3**.

The granodiorites have a relatively wide range of chemical compositions, with SiO_2 = 65.73 wt% to 69.94 wt%, Al_2O_3 = 13.04 wt% to 14.11wt%, MgO = 1.41 wt% to 1.90 wt% ($Mg^{\#}$ = 40 to 46), Fe_2O_3 = 4.67 wt% to 5.59 wt%, CaO = 0.72 wt% to 2.72 wt%, K_2O = 3.71 wt% to 4.98 wt% and Na_2O = 2.45 wt% to 4.03 wt%. They have consistent TiO_2 = 0.67 wt% to 0.81 wt%, MnO = 0.06 wt% to 0.08 wt% and P_2O_5 = 0.14 wt% to 0.16 wt%.

Table 2. Major oxides (wt%) for the felsic rocks in Guilong, Yunnan Province, China.

Sample	Rock type	SiO_2	TiO_2	Al_2O_3	Fe_2O_3	MnO	CaO	MgO	K_2O	Na_2O	P_2O_5	LOI	Total	$Mg^{\#}$	T_{Zr} (˚C)
GL-1	granodiorite	66.91	0.71	13.04	4.75	0.08	2.72	1.59	4.44	2.57	0.15	2.36	99.32	42	840
GL-2	granodiorite	67.47	0.77	14.06	5.21	0.07	0.74	1.72	4.12	4.03	0.16	1.76	100.11	42	844
GL-3	granodiorite	68.94	0.71	13.34	4.67	0.07	1.00	1.51	4.48	3.50	0.15	1.81	100.17	42	846
GL-4	granodiorite	66.82	0.67	13.57	4.70	0.07	1.81	1.56	4.18	2.84	0.14	2.75	99.11	42	857
GL-5	granodiorite	66.85	0.74	13.63	5.07	0.08	1.43	1.71	4.66	2.54	0.15	2.37	99.22	43	842
GL-6	granodiorite	67.29	0.74	13.72	5.10	0.07	0.93	1.66	4.67	2.53	0.16	2.38	99.25	42	873
GL-7	granodiorite	67.82	0.81	14.07	4.96	0.07	0.99	1.68	4.81	2.65	0.16	1.86	99.87	43	886
GL-8	granodiorite	67.53	0.75	13.56	4.96	0.06	1.04	1.41	4.79	2.57	0.16	2.36	99.18	38	853
GL-9	granodiorite	68.00	0.76	13.78	5.00	0.08	0.91	1.69	4.83	2.52	0.16	2.14	99.87	43	867
GL-10	granodiorite	68.96	0.74	13.79	5.08	0.07	1.07	1.67	4.76	2.56	0.15	1.35	100.20	42	838
GL-11	granodiorite	65.73	0.77	14.03	5.59	0.08	0.73	1.90	4.81	2.58	0.16	2.76	99.13	43	875
GL-12	granodiorite	69.11	0.75	13.95	5.05	0.06	0.72	1.52	4.41	2.99	0.16	1.42	100.13	40	839
GL-13	granodiorite	68.72	0.69	13.46	4.65	0.07	1.45	1.56	4.72	2.59	0.14	1.85	99.91	42	825
GL-14	granodiorite	68.13	0.75	13.79	4.88	0.07	0.93	1.67	4.87	2.52	0.16	2.33	100.10	43	846
GL-15	granodiorite	67.94	0.75	13.63	4.86	0.08	1.75	1.58	4.37	2.83	0.15	1.98	99.92	42	825
GL-16	granodiorite	68.46	0.72	13.35	5.35	0.08	0.97	1.65	3.71	3.48	0.15	1.99	99.91	40	840
GL-17	granodiorite	67.54	0.74	13.64	5.07	0.06	1.05	1.62	4.79	2.60	0.16	2.31	99.58	41	845
GL-18	granodiorite	66.21	0.72	13.63	5.17	0.07	1.43	1.54	4.77	2.86	0.15	2.63	99.18	42	839
GL-19	granodiorite	68.04	0.76	13.94	5.2	0.07	1.19	1.62	4.90	2.45	0.16	1.75	100.07	41	851
GL-20	granodiorite	69.13	0.74	13.61	5.11	0.08	1.19	1.66	4.44	2.67	0.15	1.45	100.22	42	835
GL-21	granodiorite	66.88	0.73	13.86	4.78	0.06	0.93	1.55	4.97	2.99	0.16	2.37	99.28	42	845
GL-22	granodiorite	67.75	0.75	13.68	5.14	0.08	1.38	1.71	4.36	2.77	0.15	2.24	100.01	42	841
GL-23	granodiorite	69.94	0.77	13.79	5.15	0.07	0.85	1.60	4.84	2.70	0.16	0.56	100.43	41	852
GL-24	granodiorite	67.65	0.72	13.84	4.84	0.06	0.90	1.58	4.96	2.58	0.15	2.12	99.39	43	839
GL-25	granodiorite	69.11	0.72	13.94	4.71	0.07	1.16	1.52	4.88	2.69	0.15	1.21	100.16	46	847
GL-26	granodiorite	69.13	0.75	14.11	5.00	0.07	1.30	1.63	4.98	2.62	0.15	0.38	100.13	45	848
GL-27	granodiorite	68.92	0.75	13.92	5.54	0.10	1.16	1.56	4.71	2.74	0.16	0.57	100.13	41	857
GSR-3	RV*	44.64	2.37	13.83	13.4	0.17	8.81	7.77	2.32	3.38	0.95	2.24	99.88	-	-
GSR-3	MV*	44.75	2.36	14.14	13.35	0.16	8.82	7.74	2.3	3.18	0.97	2.12	99.89	-	-
GSR-1	RV*	72.83	0.29	13.4	2.14	0.06	1.55	0.42	5.01	3.13	0.09	0.7	99.62	-	-
GSR-1	MV*	72.65	0.29	13.52	2.18	0.06	1.56	0.46	5.03	3.15	0.11	0.69	99.70	-	-

Note: LOI, loss on ignition. $Mg^{\#}$ = 100 × Mg/(Mg + ∑Fe) atomic ratio. "-", not caculated. T_{Zr} (˚C) is calculated from zircon saturation thermometry [33]. RV*, recommended values; MV*, measured values. The values for GSR-1 and GSR-3 are from Wang *et al*. (2003) [38].

Table 3. Trace elements (ppm) in the felsic rocks in Guilong, Yunnan Province, China.

Sample	GL-1	GL-2	GL-3	GL-4	GL-5	GL-6	GL-7	GL-8	GL-9	GL-10	GL-11	GL-12	GL-13	GL-14	GL-15	GL-16	GL-17	GL-18	GL-19	GL-20	GL-21	GL-22	GL-23	GL-24	GL-25	GL-26	GL-27	OU-6 (RV*)	OU-6 (MV*)	GBPG-1 (RV*)	GBPG-1 (MV*)
Sc	15.6	14.9	13.9	14.8	14.3	16.0	16.8	14.7	15.5	13.9	15.1	13.7	12.5	13.6	13.2	14.2	14.5	14.3	13.9	12.9	14.1	14.2	13.8	13.8	13.6	14.2	14.2	22.1	21.6	13.9	14.2
V	61.5	65.3	57.5	61.5	64.7	67.1	73.1	65.3	73.9	59.8	65.3	62	56.9	61.7	61.2	64.3	66.2	63.7	64.2	58.6	62.3	64.4	63	61.2	58.9	62.4	61	129	131	96.5	103
Cr	32.2	33.5	32.4	30.2	32.8	35.0	41.0	35.6	37.6	32.7	33.5	33.7	29.9	31.9	31.7	33.2	34.1	34.3	33.8	30.6	31.5	32.7	34.1	32	32.6	34	32.1	70.8	73.5	181	187
Ni	17.0	18.2	16.1	16.7	16.8	16.8	18.7	16	16.7	15.8	16.3	16.8	14.8	16	16.2	15.9	17	16.4	16.7	15.1	15.8	16.4	16.7	15.5	15.6	15.9	15.6	39.8	42.5	59.6	60.6
Rb	208	177	183	200	211	234	236	214	231	211	234	193	207	216	192	154	208	220	231	191	208	198	210	217	225	225	225	120	122	56.2	61.4
Sr	174	159	136	180	172	196	201	113	195	168	166	114	183	176	183	118	115	160	115	157	161	188	150	141	186	189	191	131	136	364	377
Y	37.6	42.3	38.1	39.9	39.7	42.6	43.4	43.4	40.3	38.4	39.9	41.7	37.4	39.7	40.3	42.4	54.5	42.1	41.4	37.4	42.1	41.1	41.9	40.5	37.9	39.3	41.8	27.4	26.2	18.0	17.2
Nb	13.8	15.0	13.9	13.5	14.3	14.7	15.9	15.0	15.1	14.1	15.1	14.8	13.5	14.6	13.7	14.1	14.8	14.6	14.5	13.9	14.2	14.9	14.8	14.3	14	14.5	15.7	14.8	15.3	9.93	8.74
Ba	751	679	739	751	748	832	791	645	837	802	746	605	834	826	808	626	672	780	771	738	882	727	697	811	760	795	825	477	486	908	921
Ga	17.7	18.8	16.7	18.3	19.4	20.4	19.9	18.5	19.5	18.4	20.8	18.4	17.9	18.5	17.8	17.7	18.4	18.2	18.4	17.7	17.4	19.2	18.4	18.4	18.2	18.6	18.5	24.3	26.5	18.6	20.9
La	41.7	55.6	37.7	50.9	46	53.4	50.1	45.9	44.3	39.5	37.7	42.7	42.0	39.7	44.0	42.8	48.2	43.1	40.4	40.4	42.8	58	43.5	37.8	37.3	41.8	49.2	33.0	33.1	53.0	51.0
Ce	78.8	101	72.1	93.5	85.3	98.2	95.3	85	85.5	76.2	75.5	80.1	79.6	77.3	82.5	79.6	86.8	82.7	77.3	78.5	79.4	97.7	82.1	73.5	74.3	81.2	90.8	74.4	78.0	103	105
Pr	8.95	11	8.52	10.6	9.63	11.2	10.8	10.1	9.84	8.75	8.96	9.42	9.07	9.28	9.71	9.59	10.8	9.48	9.01	9.09	9.31	10.9	9.71	8.73	8.69	9.18	10.1	7.80	8.09	11.5	11.6
Nd	33.5	40	32.2	38.5	35.4	40.8	39.9	37.6	36.0	33	33.0	35.5	34.6	34.7	36.3	36	41.3	34.9	33.9	33.6	34.8	39.4	36.8	33.2	32.7	34.3	37.5	29.0	30.6	43.3	42.4
Sm	7.10	7.65	6.59	7.78	6.94	8.21	8.35	7.61	7.45	6.78	7.19	7.06	6.68	6.96	7.19	7.53	8.42	7.35	6.89	7.08	6.91	7.59	7.23	7.05	7.04	6.93	7.47	5.92	5.99	6.79	6.63
Eu	1.07	1.28	1.08	1.26	1.07	1.27	1.14	1.02	1.05	0.97	0.92	1.02	1.02	0.96	1.17	1.15	1.23	1.12	1.08	0.97	1.13	1.34	1.06	1.14	0.92	0.96	1.11	1.36	1.35	1.79	1.69
Gd	6.65	7.29	6.54	6.75	6.59	6.78	7.06	7.11	6.58	6.39	6.32	6.72	6.56	6.59	6.84	7.32	8.27	6.96	6.78	6.50	7.34	6.86	7.22	7.00	6.12	6.35	6.90	5.27	5.50	4.74	4.47
Tb	1.15	1.22	1.09	1.25	1.17	1.31	1.34	1.23	1.21	1.07	1.22	1.16	1.07	1.15	1.15	1.26	1.4	1.20	1.14	1.10	1.2	1.2	1.21	1.17	1.14	1.15	1.21	0.85	0.83	0.6	0.59
Dy	6.42	6.65	5.96	6.69	6.39	7.08	7.08	6.62	6.76	6.17	6.73	6.34	6.02	6.39	6.32	6.59	7.87	6.58	6.49	6.14	6.5	6.48	6.75	6.46	6.42	6.33	6.65	4.99	5.06	3.26	3.17
Ho	1.39	1.45	1.32	1.46	1.37	1.54	1.56	1.48	1.46	1.35	1.47	1.42	1.32	1.41	1.41	1.44	1.74	1.46	1.39	1.34	1.45	1.41	1.43	1.43	1.39	1.4	1.46	1.01	1.02	0.69	0.66
Er	3.92	4.18	3.65	4.03	3.96	4.23	4.30	4.24	4.11	3.8	4.12	4.0	3.71	3.84	3.95	4.0	4.78	4.12	4.12	3.73	4.04	3.97	4.04	3.87	3.8	3.84	4.05	2.98	3.07	2.01	2.02
Tm	0.52	0.57	0.50	0.57	0.54	0.59	0.59	0.57	0.58	0.53	0.58	0.56	0.52	0.52	0.52	0.55	0.65	0.58	0.55	0.51	0.56	0.53	0.55	0.53	0.53	0.52	0.54	0.44	0.45	0.3	0.29
Yb	3.54	3.71	3.32	3.68	3.49	3.82	3.83	3.76	3.70	3.35	3.71	3.61	3.35	3.34	3.54	3.61	4.15	3.7	3.67	3.25	3.67	3.58	3.59	3.45	3.63	3.56	3.6	3.00	3.09	2.03	2.03
Lu	0.54	0.52	0.47	0.54	0.50	0.57	0.57	0.55	0.54	0.48	0.55	0.51	0.48	0.49	0.51	0.51	0.58	0.53	0.53	0.49	0.51	0.52	0.52	0.50	0.50	0.51	0.52	0.45	0.47	0.31	0.31
Hf	5.32	4.68	4.62	5.65	4.54	5.74	6.44	4.79	5.51	4.09	5.81	4.01	3.88	4.38	3.92	4.38	4.42	4.62	4.85	4.18	4.58	4.39	4.73	4.07	4.71	4.8	5.09	4.7	4.86	6.07	5.93
Zr	201	180	186	218	175	224	256	190	212	158	227	156	146	172	150	168	174	173	183	155	179	170	181	161	177	180	195	174	183	232	224
Ta	1.23	1.28	1.15	1.18	1.18	1.30	1.32	1.28	1.26	1.19	1.29	1.21	1.16	1.21	1.18	1.18	1.24	1.24	1.25	1.17	1.20	1.23	1.24	1.21	1.27	1.24	1.3	1.06	1.02	0.4	0.46
Pb	76.1	46.7	48.1	89.4	65.5	102	91.4	324	88.2	78.4	33.0	183	68.6	129	75.5	42.7	107	53.2	126	194	73.8	80.1	58.6	107	65.2	74.0	50.7	28.2	32.7	14.1	14.5
Th	21.7	24.2	22.2	23.0	23.2	23.8	24.1	24.5	23.2	23.5	24.5	23.9	22.4	23.6	23.2	22.8	24.2	24.1	23.7	22.4	23.1	23.7	23.3	23.6	24.2	24.3	24.8	11.5	13.9	11.2	11.4
U	4.86	5.34	4.7	5.08	4.9	5.30	5.31	5.07	5.13	4.79	5.27	4.94	4.69	4.92	4.85	4.75	5.11	5.24	5.07	4.92	4.9	4.98	5.0	4.91	5.09	5.11	5.24	1.96	2.19	0.90	0.99
dEu	0.48	0.53	0.50	0.53	0.48	0.52	0.45	0.42	0.46	0.45	0.42	0.45	0.47	0.43	0.51	0.47	0.45	0.48	0.48	0.44	0.49	0.57	0.45	0.49	0.43	0.44	0.47				

The granodiorites are relatively high in total alkalis, with $K_2O + Na_2O$ ranging from 7.02 wt% to 8.15 wt%. All granodiorites in the calc-alkaline field are plotted on the Total Alkali-Silica (**TAS**) diagram (**Figure 4(a)**). All samples also straddle the shoshonitic series in the Na_2O vs K_2O plot (**Figure 4(b)**). In the plot of the molar ratios of $Al_2O_3/(Na_2O + K_2O)$ and $Al_2O_3/(CaO + Na_2O + K_2O)$, the rocks are mostly peraluminous, except for one sample falling the metaluminous field (**Figure 4(c)**). The granodiorites display almost unchanged TiO_2, Al_2O_3, Fe_2O_3, MgO, CaO, $Na_2O + K_2O$, MnO, P_2O_5, Rb, Cr and Ni, relatively decreasing Zr and increasing SiO_2. They have no correlations among Sr, Ba and SiO_2 (**Figures 5** and **6**).

All granodiorites are characterized by Light Rare Earth Element (**LREE**) enrichment and Heavy Rare Earth Element (**HREE**) depletion, with a wide range of $(La/Yb)_N$ values (7.29 to 11.62) and slight negative Eu anomalies ($Eu/Eu^* = 0.42$ to 0.57) (**Table 3** and **Figure 7(a)**). In the primitive mantle-normalized trace element diagrams, the granodiorites show enrichment in Large Ion Lithophile Elements (**LILE**) (*i.e.*, Rb, Pb and U) and depletion in Ba, Sr and High Field Strength Elements (HFSE) (*i.e.*, Nb, Ta, P and Ti) (**Figure 7(b)**).

4.3. Sr-Nd and Pb Isotopes

Sr-Nd isotopic data have been obtained from representative granodiorite samples (**Table 4**). The felsic rocks show uniform $(^{87}Sr/^{86}Sr)_i$ values, ranging from 0.7231 to 0.7237 and relatively little variation in initial. ε_{Nd} (*t*) values from –29.1 to –30.4, suggesting an enriched source region. The Sr-Nd isotopic compositions (**Figure 8**) are also comparable with the upper crust.

5. Discussion

5.1. Mantle Contribution

Currently, the interaction between crust and mantle is very important for the genetic investigation of granitoid rocks. Previous studies suggest that mantle contribution (e.g., material and energy) during granitoid rock formation cannot be ignored [19-21].

The REE of the granodiorites [$\Sigma REE = 181^\circ$ ppm to 242° ppm, $(La/Yb)_N = 7.29$ to 11.62, $\delta Eu = 0.42$ to 0.57] has some visible differences with that of granitoid rocks formed by re-melting of the continental crust with high maturity, such as Suidong intrusion in Southern China [$\Sigma REE = 169^\circ$ ppm to 268° ppm, $(La/Yb)_N = 6.44$ to 10.74, $\delta Eu = 0.14$ to 0.31 [22]. However, the REE can be comparable with that of syntactic-type granitic rocks involving obvious mantle material in their petrogenesis in southern China, e.g., Wuping intrusion [$\Sigma REE = 103^\circ$ ppm to 395° ppm, $(La/Yb)_N = 5.3$ to 38.7, $\delta Eu = 0.34$ to 0.56] [23] and Longwo intrusion [$\Sigma REE = 103^\circ$ ppm to 196° ppm, $(La/Yb)_N = 4.5$ to 35.7, $\delta Eu = 0.41$ to 0.62] [24].

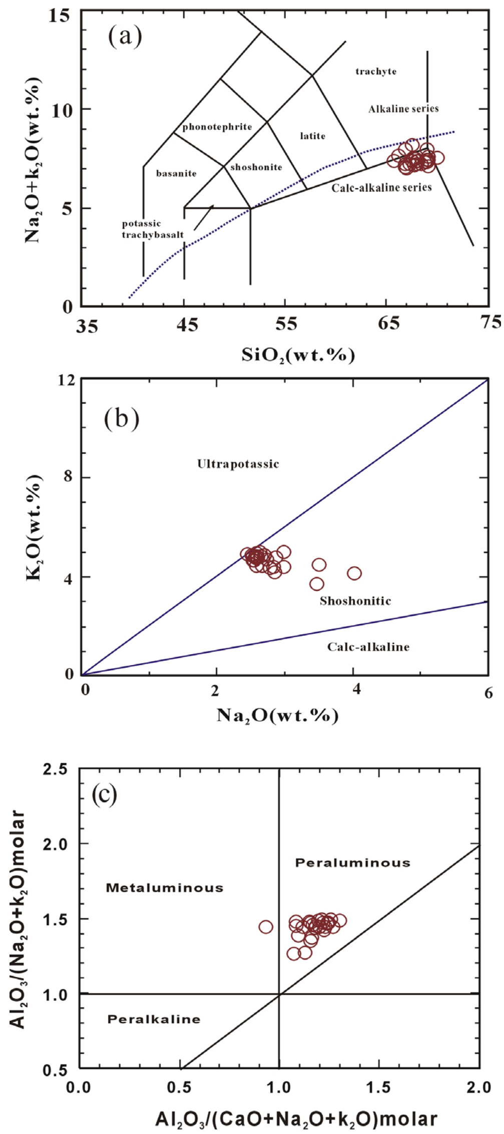

Figure 4. Classification of the granodiorites in Southeastern Yunnan province based on three diagrams. (a) TAS diagram. All major elemental data have been recalculated to 100% on a LOI-free basis [34-35]. (b) K_2O vs Na_2O diagram. The granodiorites are shown to be shoshonitic [36]. (c) $Al_2O_3/(Na_2O + K_2O)$ molar vs $Al_2O_3/(CaO + Na_2O + K_2O)$ molar plot. Most samples fall in the peraluminous field. However, one sample straddles the metaluminous field.

The granodiorites in the present study have relatively higher compatible element contents ($V = 58.6^\circ$ ppm to 73.1° ppm, $Cr = 29.9^\circ$ ppm to 41.0° ppm, $Ni = 14.8^\circ$ ppm to 18.7° ppm) than some granitic rocks formed by the interaction of crust and mantle in the Yangtze River and southern China (Wuping biotite monzogranite [23]; granodiorites in Longwo [24,25]). In addition, the high $Mg^\#$ (43 - 46; **Table 2**) of the rocks agrees with interaction of crust and mantle. Simutaneously, the Sr-Nd isotopic signatures

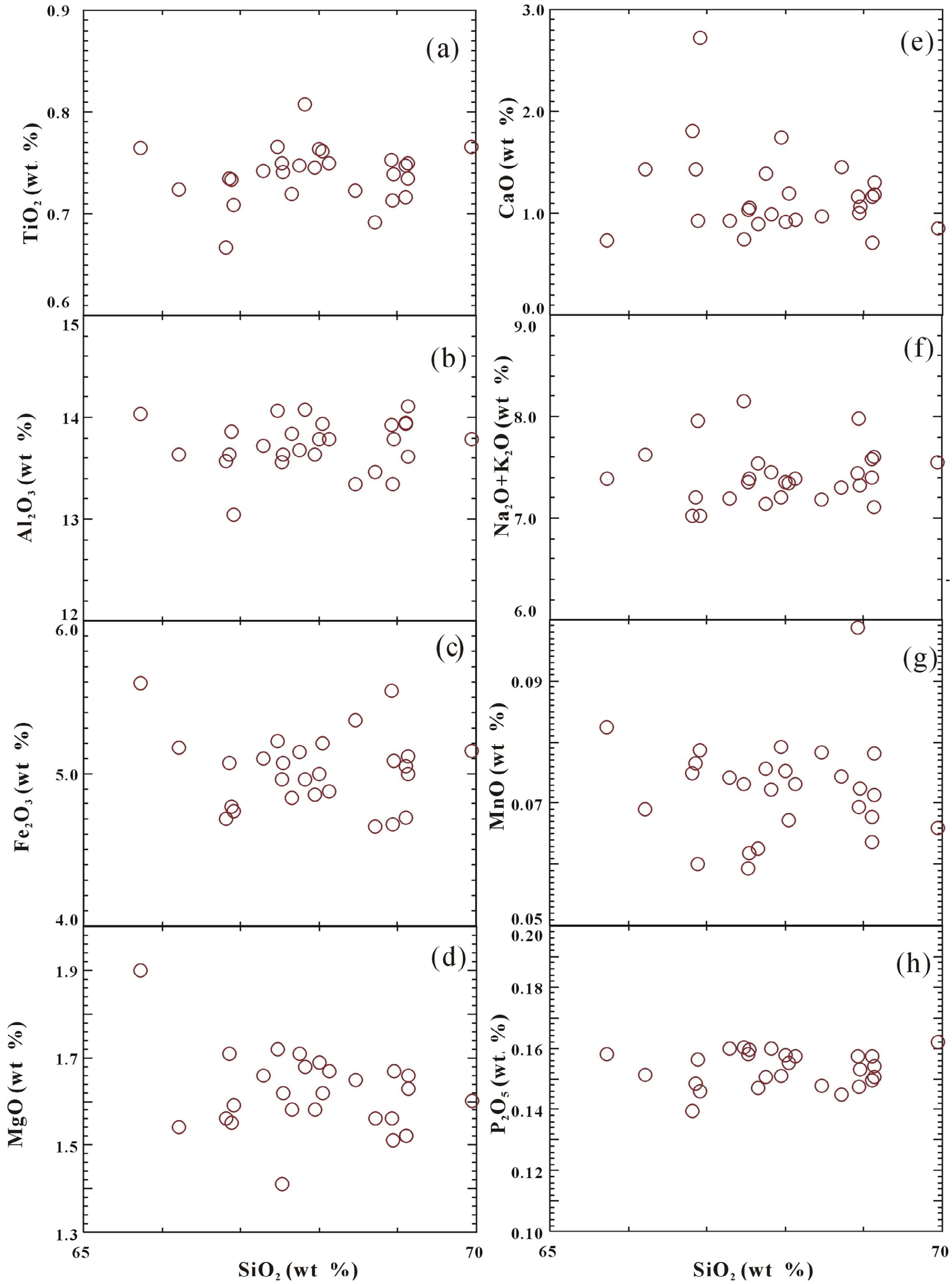

Figure 5. Selected variation diagrams of major elemental oxides vs SiO_2 plots for the felsic rocks in Southeastern Yunnan Province.

of the granodiorites are comparable with those in the associated mafic dykes (lamprophyres) in the study area (**Figure 1**).

In summary, this evidence indicates that evident mantle materials contributed to the diagenesis of Guilong granodiorites in Yunnan Province.

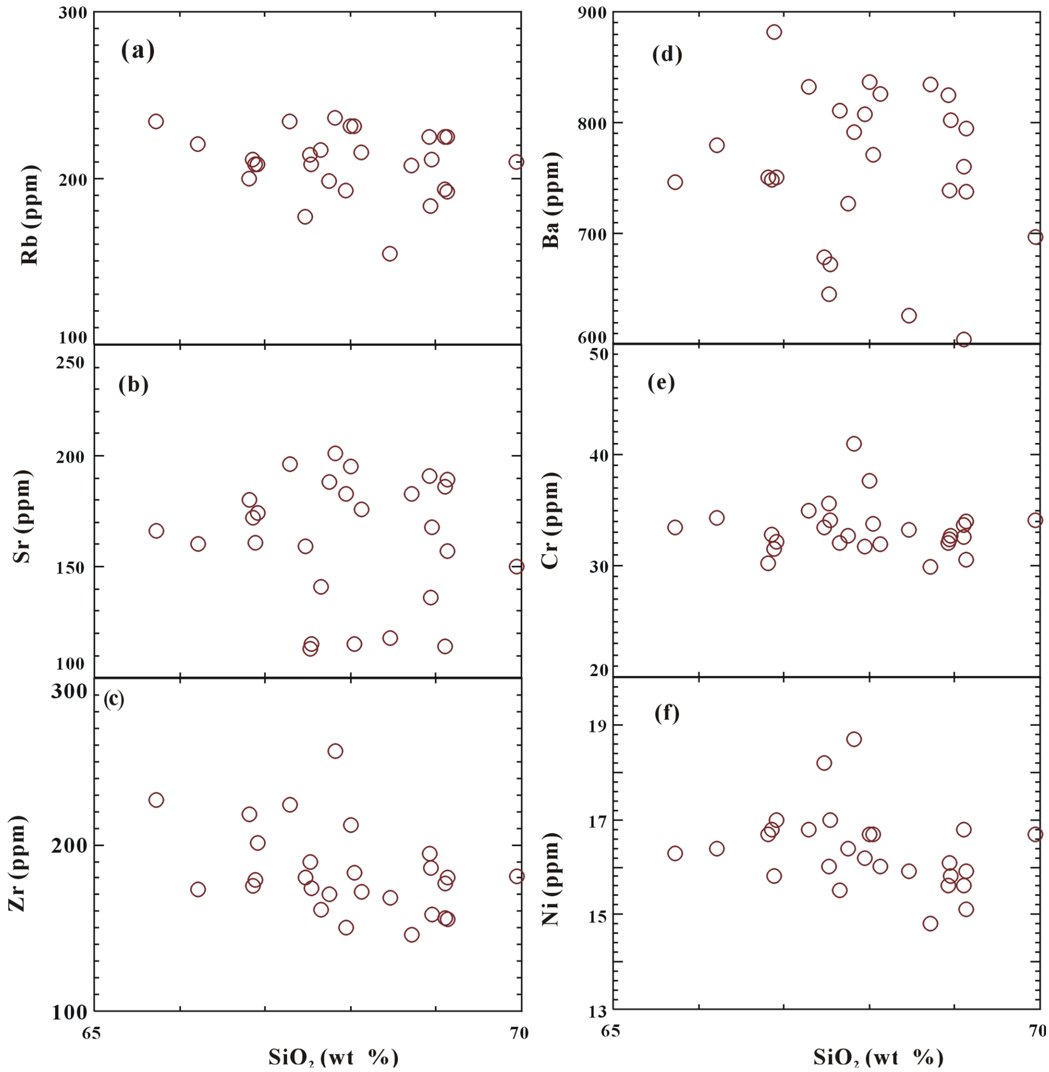

Figure 6. Selected variation diagrams of trace elements vs SiO_2 plots for the felsic rocks in Southeastern Yunnan Province.

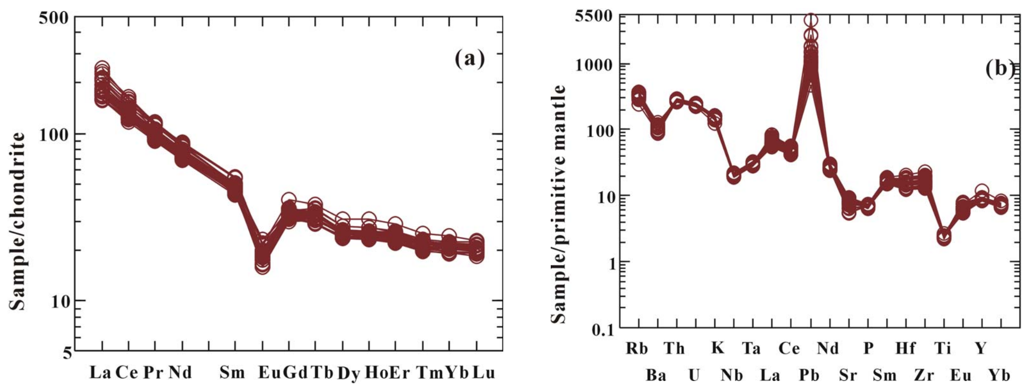

Figure 7. (a) Chondrite-normalized REE diagrams; (b) Primitive mantle-normalized trace element spidergrams for the granodiorites in Southeastern Yunnan Province. The normalization values are from Sun and McDonough (1989) [37].

5.2. Crustal Contamination

Assimilation, crystal fractionation (**AFC**), or magma mixing is usually postulated to explain the occurrence of comagmatic felsic rocks [26-29]. AFC and magma mixing result in a positive correlation between SiO_2 and ε_{Nd} (t) values and a negative correlation between SiO_2 and

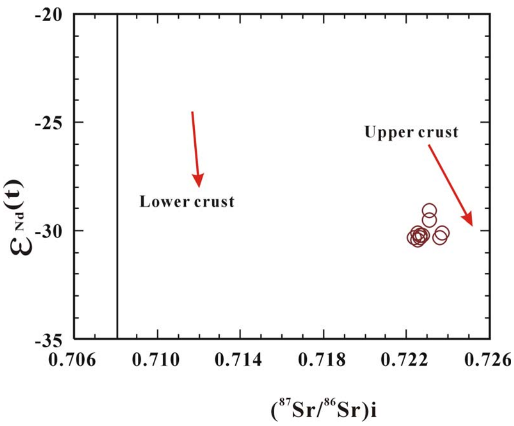

Figure 8. Initial $^{87}Sr/^{86}Sr$ vs ε_{Nd} (*t*) diagram for the felsic rocks in Southeastern Yunnan Province.

$(^{87}Sr/^{86}Sr)_i$ ratios (**Figure 9**). However, these features are not observed in the studied granodiorites, indicating that magma evolution is insignificantly affected by crustal contamination or magma mixing. Therefore, the geochemical and Sr-Nd isotopic signatures of the granodiorites are mainly inherited from an enriched source.

5.3. Origin of the Rocks and Fractional Crystallization

The granodiorites have relatively low Al_2O_3/TiO_2 (17.4 to 20.3), suggesting that the temperature of partial melting is high (>875˚C [30]). Moreover, felsic rocks have low Sr (113˚ ppm to 201˚ ppm) and high Yb (3.25˚ ppm to 4.15˚ ppm), with the lower Sr and higher Yb feature. In addition, the granodiorites are provided with low $(La/Yb)_N$ (7.29 to 11.62) and negative slight Eu negative (δEu = 0.42 to 0.57) **(Table 3)**. Hence, the rocks resulted from relatively low pressure (<1.2˚ Gpa) and a shallow source [31].

For the studied felsic samples, the negative Nb, Ta and Ti anomalies in all rocks (**Figure 7(b)**) agree with the fractionation of such Fe-Ti oxides as rutile and ilmenite. The relatively negative Ba, Sr and Eu anomalies of the rocks (**Figures 7(a)** and **(b)**) imply the fractionation of potassium feldspar and plagioclase.

Besides above, the granodiorites have characterized Sr-Nd isotopic compositions ($(^{87}Sr/^{86}Sr)_i$ = 0.7231 - 0.7237, ε_{Nd} (*t*) = –29.1 - –30.4). The geochemistry feature all indicate that the granodiorites were derived from partial melting of crust-derived sedimentary rocks. Moreover, interaction of crust and mantle occurred during origin of the granodiorites.

The granodiorites show relatively decreasing Zr with increasing SiO_2 (**Figure 6(c)**). This result indicates that zircon was saturated in the magma, which was also controlled by fractional crystallization [32]. Zircon saturation thermometry [33] provides a simple and robust

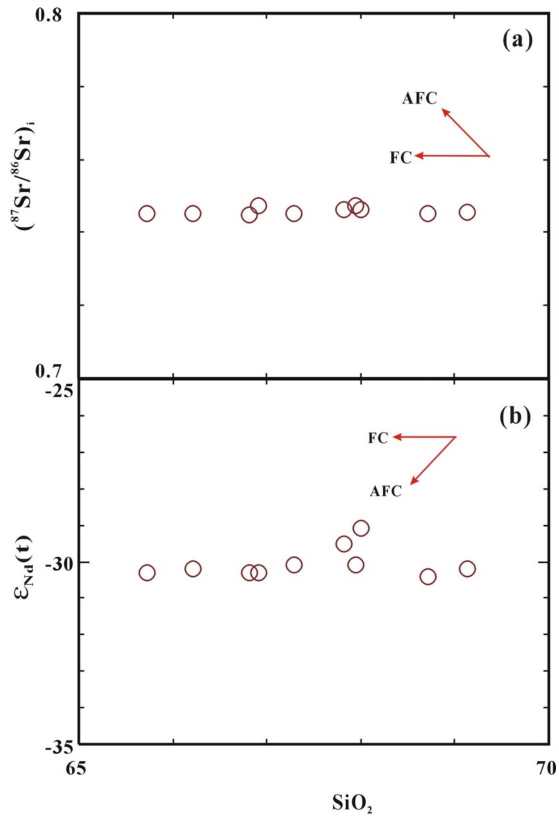

Figure 9. Plots of (a) initial $^{87}Sr/^{86}Sr$ ratio and (b) ε_{Nd} (*t*) value vs SiO_2 for the felsic rocks in Southeastern Yunnan province, indicating crystal fractionation. FC, fractional crystallization; AFC, assimilation and fractional crystallization.

means of estimating magma temperatures from bulk-rock compositions. The calculated zircon saturation temperatures (T_{Zr}) of felsic rocks are 825˚C to 886˚C (**Table 2**), representing the crystallization temperature of the magma.

6. Conclusions

Based on geochronological, geochemical and Sr-Nd isotopic studies, the following conclusions are drawn:

1) Granodiorites were formed at 252.5 ± 1.0 based on **LA-ICP-MS** U-Pb zircon dating. The rocks resulted from post-collision magmatism.

2) Felsic rocks came from a crustal source. The fractionation of K-feldspar, plagioclase, ilmenite, or rutile, among others, resulted in granodiorites with negligible crustal contamination. The zircon saturation temperatures (T_{Zr}) of the granodiorites range from 825˚C to 875˚C, approximately representing the crystallization temperature of the magma.

7. Acknowledgements

The present research was supported by the Knowledge Innovation Project (KZCX2-YW-111-03) and the National Nature Science Foundation of China (40773020, 40972071, 90714010 and 40634020). The authors gratefully acknowledge Lian Zhou for helping analyze the Sr-Nd isotopes and Yongsheng Liu and Zhaochu Hu for their help with the LA-ICP-MS zircon U-Pb dating.

REFERENCES

[1] Southwest Geological Exploration Corporation, "Geology of Tin Deposits in Gejiu," Metallurgical Industry Publishing House, Beijing, 1984.

[2] J. Chen, C. Hall and C. J. Stanley, "Tin-Bearing Skarns of South China: Geological Setting and Mineralogy," *Ore Geology Reviews*, Vol. 7, No. 3, 1992, pp. 225-248. doi:10.1016/0169-1368(92)90006-7

[3] Y. Q. Zhuang, R. Z. Wang and J. M. Yin, "Geology of the Gejiu Tin-Copper Olymetallic Deposit," Geological Publishing House, Beijing, 1996.

[4] Z. W. Jiang, N. H. S. Oliver, T. D. Barr W. L. Power and A. Ord, "Numerical Modeling of Fault-Controlled Fluid Flow in the Genesis of the Deposits of the Malage Ore District, Gejiu Mining District, China," *Economic Geology*, Vol. 92, No. 2. 1997, pp. 228-247. doi:10.2113/gsecongeo.92.2.228

[5] G. P. Mo, "Genetic Type of Granites in Gejiu Super Large Tin Polymetallic Deposit," *Mineral Resources and Geology*, Vol. 20, No. 45, 2006, pp. 413-417.

[6] Y. B. Cheng and J. W. Mao, "Age and Geochemistry of Granites in Gejiu Area, Yunnan Province, SW China: Constraints on Their Petrogenesis and Tectonic Setting," *Lithos*, Vol. 120, No. 3-4, 2010, pp. 258-276. doi:10.1016/j.lithos.2010.08.013

[7] The Second Geological Team of Yunnan Geological and Mineral Urea, "The Report of Prospecting at the Region of Bainiuchang in Mengzi County, Yunnan Province," Yunnan Ecological and Mineral Bureau, Mengzi County, 1990.

[8] Z. Y. Gao, "On the Genesis of the Bainiuchang Silver-Polymetallic Deposit in Mengzi," *Yunnan Geology*, Vol. 15, No. 4, 1996, pp. 91-102.

[9] X. M. Chen, Z. Lin and F. H. Xie, "Geological and Geochemical Characteristics of the Bainiuehang Super Large Silver Polymetallic Deposit of Supreme Posed Mineralization, Yunnan Province," *Scientia Geologica Sinica*, Vol. 33, No. 1, 1998, pp. 115-123.

[10] X. B. Li, J. S. Liu, H. P. Zhang and G. Ma, "The Analysis to Ore-Controlling Factors of the Bainiuehang Ag Polymetallic Deposit of Mengzi County in Yunnan Province," *Contribution to Geology and Mineral Resources Research*, Vol. 20, No. 2, 2005, pp.111-114.

[11] H. J. Xie, C. H. Zhu, Q. Zhang, Q. Wang and L. W. Fan, "Sulfur Isotopic Composition of the Bainiuchang Super Large Ag Polymetallic Deposit, Yunnan Province, China: Implications for the Source of Sulfur in Ore Forming Fluids," *Chinese Journal of Geochemistry*, Vol. 28, No. 3, 2009, pp. 284-292. doi:10.1007/s11631-009-0284-6

[12] L. Ye, N. J. Cook, C. L. Ciobanu, Y. P. Liu, Q. Zhang, T. G. Liu, W. Gao, Y. L. Yang and L. Danyushevskiy, "Trace and Minor Elements in Sphalerite from Base Metal Deposits in South China: A La-Icpms Study," *Ore Geology Reviews*, Vol. 39, No. 4, 2011, pp. 188-217. doi:10.1016/j.oregeorev.2011.03.001

[13] C. H. Zhu, Q. Zhang, S. X. Shao and D. P. Wang, "Origin of Bainiuchang Liver-Polymetallic Deposit in Yunnan, China," *Global Geology*, Vol. 25, No. 4, 2006, pp. 353-359.

[14] C. H. Zhu, Q. Zhang, S. X. Shao, X. Q. Zhu and D. Q. Wang, " Lead Isotopic Composition and Lead Source in the Bainiuchang Ag-Polymetallic Deposit, Yunnan Province, China," *Acta Geologica Sinica*, Vol. 82, No. 5, 2008, pp. 845-857.

[15] H. L. Yuan, S. Gao, X. M. Liu, H. M. Li, D. Gunther and F. Y. Wu, "Accurate U-Pb Age and Trace Element Determinations of Zircon by Laser Ablation-Inductively Coupled Plasma Mass Spectrometry," *Geostandards Newsletter*, Vol. 28, No. 3, 2004, pp. 353-370. doi:10.1111/j.1751-908X.2004.tb00755.x

[16] T. Andersen, "Correction of Common Lead in U-Pb Analyses That Do Not Report ^{204}Pb," *Chemical Geology*, Vol. 192, No. 1-2, 2002, pp. 59-79. doi:10.1016/S0009-2541(02)00195-X

[17] K. R. Ludwig, "User's Manual for Isoplot/Ex, Version 3.00. A Geochronological Toolkit for Microsoft Excel," *Berkeley Geochronology Center Special Publication*, Vol. 4, No. 2, 2003, pp. 1-70.

[18] L. Qi, J. Hu and D. C. Grégoire, "Determination of Trace Elements in Granites by Inductively Coupled Plasma Mass Spectrometry," *Talanta*, Vol. 51, No. 6, 2000, pp. 507-513.

[19] H. E. Huppert and R. S. J. Sparks, "The Generation of Granitic Magmas by Intrusion of Basalt into Continental Crust," *Journal of the Petrology*, Vol. 29, No. 3, 1998, pp. 599-624.

[20] C. Annen and R. S. J. Sparks, "Effects of Repetitive Emplacement of Basaltic Intrusions on Thermal Evolution and Melt Generation in the Crust," *Earth Planetary Science Letters*, Vol. 203, No. 3-7, 2002, pp. 937-955.

[21] F. Y. Wu, X. H. Li and J. H. Yang, "Discussions on the Petrogenesis of Granites," *Acta Petrologica Sinica*, Vol. 23, No. 6, 2007, pp. 1217-1238.

[22] H. F. Ling, W. Z. Shen and P. Deng, "Age, Geochemistry and Petrogenesis of the Sundong Granite, Northern Guangdong Province," *Acta Petrologica Sinica*, Vol. 20, No. 3, 2004, pp. 413-424.

[23] J. H. Yu, X. M. Zhou and L. Zhao, "Mantle-Crust Interaction Generating the Wuping Granites: Evidence from Sr-Nd-Hf-U-Pb Isotopes," *Acta Petrologica Sinica*, Vol. 21, No. 3, 2005, pp. 651-664.

[24] J. S. Qiu, J. Hu and B. I. A. McInnes, "Geochronology, Geochemistry and Petrogenesis of the Longwo Granodioritic Pluton in Guangdong Province," *Acta Petrologica Sinica*, Vol. 20, No. 6, 2004, pp. 1363-1374.

[25] S. Y. Jiang, L. Li, B. Zhu, X. Ding, Y. H. Jiang, L. X. Gu and P. Ni, "Geochemical and Sr-Nd-Hf Isotopic Compositions of Granodiorite from the Wushan Copper Deposit,

Jiangxi Province and Their Implications for Petrogenesis," *Acta Petrologica Sinica*, Vol. 24, No. 8, 2008, pp. 1679-1690.

[26] D. J. DePaolo, "Trace Element and Isotopic Effects of Combined Wallrock Assimilation and Fractionation Crystallization," *Earth and Planetary Science Letters*, Vol. 53, No. 2, 1981, pp. 189-202. doi:10.1016/0012-821X(81)90153-9

[27] C. W. Devey and K. G. Cox, "Relationships between Crustal Contamination and Crystallization in Continental Flood Basalt Magmas with Special Reference to the Deccan Traps of the Western Ghats, India," *Earth and Planetary Science Letters*, Vol. 84, No. 1, 1987, pp. 59-68. doi:10.1016/0012-821X(87)90176-2

[28] J. S. Marsh, "Geochemical Constraints on Coupled Assimilation and Fractional Crystallization Involving Upper Crustal Compositions and Continental Tholeiitic Magma," *Earth Planetary Science Letter*, Vol. 92, No. 1, 1989, pp. 78-80. doi:10.1016/0012-821X(89)90021-6

[29] B. Mingram, R. B. Trumbull, S. Littman and H. Gertenberger, "A Petrogenetic Study of Anorogenic Felsic Magmatism in the Cretaceous Paresis Ring Complex, Namibia: Evidence for Mixing of Crust and Mantle-Derived Components," *Lithos*, Vol. 54, No. 1-2, 2000, pp. 1-22. doi:10.1016/S0024-4937(00)00033-5

[30] P. J. Sylvester, "Post-Collisional Strongly Peraluminous Granites," *Lithos*, Vol. 45, No. 1-4, 1998, pp. 29-34. doi:10.1016/S0024-4937(98)00024-3

[31] Q. Zhang, Y. Wang and C. D. Li, "Granite Classification on the Basis of Sr and Yb Contents and Its Implications," *Acta Petrologica Sinica*, Vol. 22, No. 9, 2006, pp. 2249-2269.

[32] X. H. Li, Z. X. Li, W. X. Li, Y. Liu, C Yuan, G. J. Wei and C. S. Qi, "U-Pb Zircon, Geochemical and Sr-Nd-Hf Isotopic Constraints on Age and Origin of Jurassic I and A-Type Granites from Central Guangdong, SE China: A Major Igneous Event in Response to Foundering of a Subducted Flat-Slab," *Lithos*, Vol. 96, No. 2, 2007, pp. 186-204. doi:10.1016/j.lithos.2006.09.018

[33] E. B. Watson and T. M. Harrison, "Zircon Saturation Revisited: Temperature and Composition Effects in a Variety of Crustal Magma Types," *Earth and Planetary Science Letters*, Vol. 64, No. 2, 1983, pp. 295-304. doi:10.1016/0012-821X(83)90211-X

[34] E. A. K Middlemost, "Naming Materials in the Magma/Igneous Rock System," *Earth-Science Reviews*, Vol. 37, No. 3-4, 1994, pp. 215-224. doi:10.1016/0012-8252(94)90029-9

[35] R. W. Le Maitre, "Igneous Rocks: A Classification and Glossary of Terms," 2nd Edition, Cambridge University Press, Cambridge, 2002.

[36] E. A. K. Middlemost, "A Simple Classification of Volcanic Rocks," *Bulletin of Volcanology*, Vol. 36, No. 2, 1972, pp. 382-397. doi:10.1007/BF02596878

[37] S. S. Sun and W. F. McDonough, "Chemical and Isotopic Systematics of Oceanic Basalts: Implications for Mantle Composition and Processes. Magmatism in the Ocean Basins," In: A. D. Saunders and M. J. Norry, Eds., Geological Society Special Publication, London, 1989, pp. 313-345.

[38] Y. M. Wang, Y. S. Gao, H. M. Han and X. H. Wang, "Practical Handbook of Reference Materials for Geoanalysis," Geological Publishing House, Beijing, 2003.

[39] M. Thompson, P. J. Potts, J. S. Kane and S. Wilson, "An International Proficiency Test for Analytical Geochemistry Laboratories-Report on Round 5 (August 1999)," *Geostandards and Geoanalytical Research*, Vol. 24, No. 1, 2000, pp. E1-E28.

[40] P. J. Potts and J. S. Kane, "International Association of Geoanalysts Certificate of Analysis: Certified Reference Material OU-6 (Penrhyn Slate)," *Geostandards and Geoanalytical Research*, Vol. 29, No. 2, 2005, pp. 233-236. doi:10.1111/j.1751-908X.2005.tb00895.x

[41] R. H. Steiger and E. Jäger, "Subcommission on Geochronology; Convention on the Use of Decay Constants in Geochronology and Cosmochronology," *Earth and Planetary Science Letters*, Vol. 36, No. 3, 1977, pp. 359-362.

[42] G. W. Lugmair and K. Harti, "Lunar Initial $^{143}Nd/^{144}Nd$: Differential Evolution of the Lunar Crust and Mantle," *Earth and Planetary Science Letters*, Vol. 39, No. 3, 1978, pp. 349-357. doi:10.1016/0012-821X(78)90021-3

